Bulletin of Earth Sciences of Thailand

Investigation of Morphotectonics along the Mae Chan and Nam Ma Fault Zones, Thailand-Laos-Myanmar Borders

Tassana Jadeanan and Santi Pailoplee*

Center of Excellence for Morphology of Earth Surface and Advanced Geohazards in Southeast Asia (MESA RU), Department of Geology, Faculty of Science, Chulalongkorn University, Bangkok 10330, Thailand
* Corresponding author e-mail: Pailoplee.S@gmail.com

Abstract

The Mae Chan and Nam Ma faults are well-known as active faults in mainland Southeast Asia, located at the borders of Thailand, Laos, and Myanmar. This study used the morphotectonic analysis of various geomorphic indices to evaluate relative tectonic activity in the study area. A digital elevation model from the Advanced Spaceborne Thermal Emission Radiometer (ASTER) was chosen to create the watershed delineation by analyzing the geological data and hydrogeological model. The total hydrogeological areas are 38 basins. The six geomorphic indices applied to this study included mountain front sinuosity (SMF), valley floor width to height ratio (VF), stream length gradient index (SL), basin shape index (BS), basin asymmetry index (AF), and basin hypsometric index (HI) for the categorization of the relative index of active tectonics (RIAT) through the use of geographic information systems (GIS). The analysis found that lineament patterns of the Mae Chan and Nam Ma faults mainly trend in the NE-SW direction. The RIAT results in the study area are divided into three classes: class-1 (inactive 4.79% of the area), class-2 (moderately active 34.92% of the area), and class-3 (very active 60.29% of the area). Most morphometric analysis generally indicates that tectonics influence this area more than erosion. Finally, the overall geomorphic outputs of recent seismicity support the active tectonic control over this area.

Keywords: Tectonic; Seismotectonic; Morphotectonic analysis; Geomorphic indices; Mae Chan fault zone; Nam Ma fault zone.

1. Introduction

The core of tectonic geomorphology is represented by the relationship between tectonic processes that tend to build topography and surface processes that tend to tear them down. Over the last few decades, innovative methodology of new techniques for determining the age of landscape features, assessing the mechanisms and rate of geomorphic processes, and defining rates of crustal movement has helped revitalize the field of tectonic geomorphology. To measure the amount of deformation affected by tectonic processes, it is necessary to indicate the geomorphic markers or landscape features, such as marine or fluvial terraces, that can be used to track deformation on the land surfaces in terms of planar or linear features with known geometry. Faulting or folding can deform such markers (Burbank & Anderson, 2011). However, the best geomorphic markers are readily recognizable landforms, surfaces, or linear trends.

Drainage patterns are controlled by the underlying geology, slope, and topography. Moreover, climate change is also influential. Accordingly, many influential factors are key, which is helpful in the interpretation of geomorphic features and understanding of structural and lithological control of landform evolution. In addition, the impact of tectonics on landform development and geomorphic processes in active tectonic regions can be qualitative and quantitative analyzed by studying the drainage pattern (Bull, 2011; El Hamdouni et al., 2008; Jackson et al., 1998; Keller & Pinter, 1996, 2002) and drainage anomalies are the deviation of present drainage pattern from the regional

patterns, can be provided on tectonic deformation (Ahmad et al., 2014; Clark et al., 2004; Howard, 1967).

Geomorphic indices are defined as quantitative measurements of landscape shape. The different landforms can be characterized in terms of size, elevation (maximum, minimum, or average), and slope. A comparison of the calculated parameters may be useful for identifying a particular characteristic of an area, such as the level of tectonic activity. They are reflective of the interaction of tectonic processes, climate change, rock resistance, and the influence of structure, resulting in landscape evolution (Keller & Pinter, 2002; Bhatt et al., 2008).

The earthquakes around northern Thailand are mostly recorded as moderate magnitude (3-6 on the Richter scale), and several large earthquakes (magnitude ≥ 6) from the instrumental records. Based on the detected earthquake data, the Mae Chan fault zone (MCFZ) and Nam Ma fault zone (NMFZ) can be identified as active fault fields (Morley, 2004, 2007). Both are a left-lateral strike-slip fault that is a clear lineament by a remote sensing investigation with a length of more than 200 kilometers in a northeast-southwest direction. However, the largest earthquakes recorded have occurred in Myanmar with a magnitude of 6.2 near the border of three countries on NMFZ (Ornthammarath, 2012).

In this paper, we focus on the movement record along MCFZ and NMFZ by using remote sensing techniques, GIS, and geomorphic index as basic tools to identify and analyze the characteristic morphotectonic landforms that result from fault movements. Moreover, based on this analysis, we can evaluate the tectonic activities in our study area, which is entirely some of the Sarawin and Mae Khong River basins along the Thailand, Laos, and Myanmar borders. The GPS coordinates between latitude 19°30’ to 22°20’ north and 99°60’ to 102°20’ east, covering a surface area of approximately 99.45 km^2 (Figure 1).

The regional topography of MCFZ and NMFZ is mainly composed of complex mountainous areas that serve as the catchment basin of the Sarawin River in the west and the Mae Khong River in the east. They pass through many cities, flowing from the north to the south. It is surrounded by high mountain ranges, a strongly incised plateau, and a piedmont. The main plain covers the southwest area, which is in the central part of Chiang Rai province. Therefore, the altitude is about 257 to 1,760 meters above sea level.

However, these studies offer some understanding of the existence and characteristics of structures and seismic activity. Nonetheless, due to their regional focus, the exact locations of areas experiencing abnormal uplift or erosion are still uncertain. The paper aims to access tectonic activity areas along the Mae Chan and Nam Ma fault zones by using principal geomorphic and morphometric indices. The different indices are utilized for the establishment of a relative index of active tectonics (RIAT) and for classifying the basins and sub-basins into different classes from relatively low to the highest tectonic activity. The current work utilizes integrated morphotectonics and morphometric analyses, which are further supported by the seismicity pattern of the recent past.

2. Geomorphic Index

Basins were analyzed through a set of tectonic geomorphic indices to infer tectonic activity and its spatial variation. The base data was generated using the ASTER Global Digital Elevation Model (ASTER GDEM) with 30 meters of resolution. This DEM was used to define and extract basin drainage and stream network data together with the Hydrology toolset of the Spatial Analyst Tools ArcGIS toolbox. This step corrects the error of sources by filling sinks or holes in the DEM. Then, to define the hydrologic characteristics, the flow direction, the flow accumulation, the stream network, and the catchment area (drainage basin) were computed from every cell in the raster. All processes are with ArcGIS software. The outputs are in raster format and then converted to shapefile format. After that, six geomorphic indices factors were analyzed spatially covering MCFZ and NMFZ that are mountain front sinuosity index (SMF), valley floor width to height ratio index (VF), stream length gradient index (SL), basin shape

index (BS), basin asymmetry index (AF) and basin hypsometric index (HI).

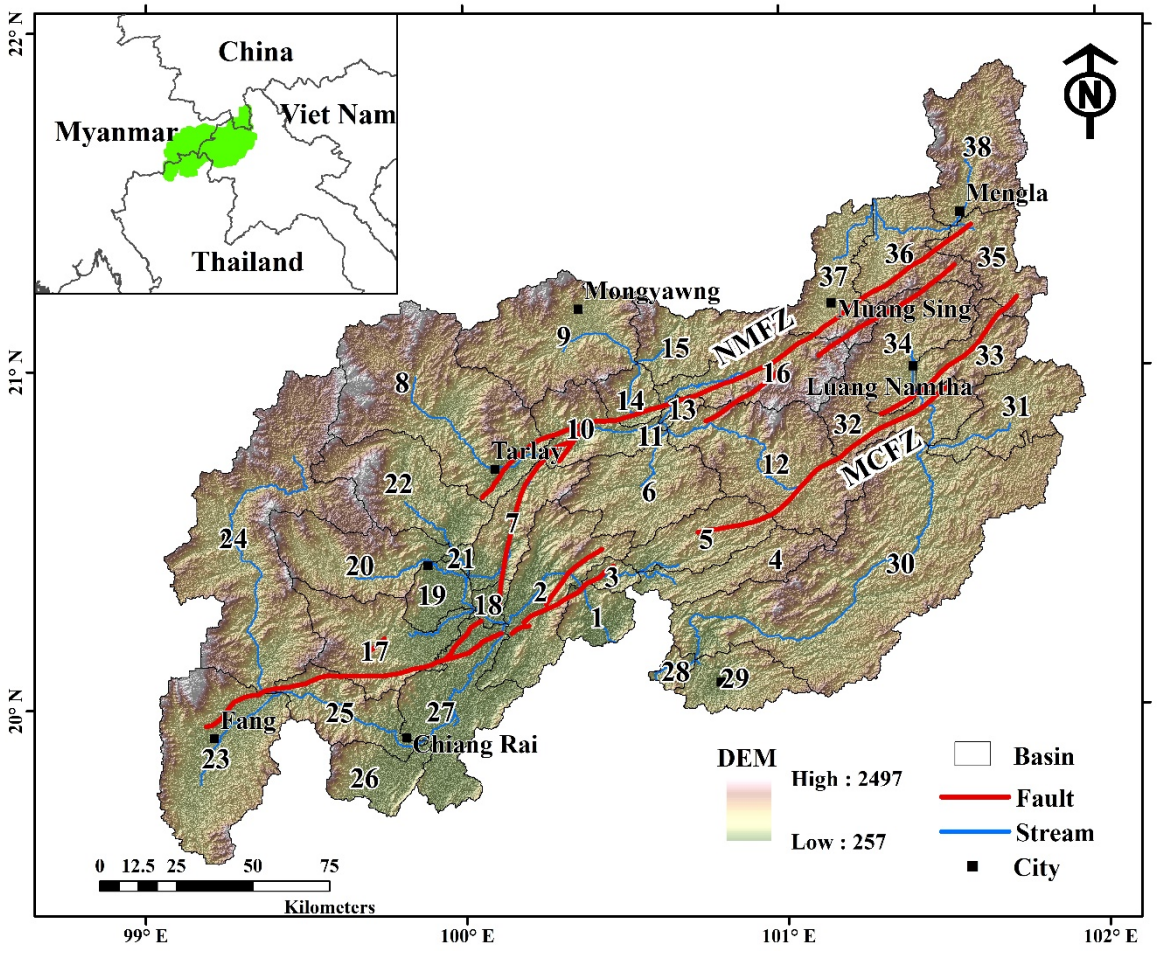

Figure 1. Map of MCFZ and NMFZ (red line) along Thailand-Laos-Myanmar borders showing the spatial distribution of topography analyzed by Digital Elevation Model (DEM) data with the main city (black square) and basins with the reference numbers.

2.1. Mountain front sinuosity

Mountainfront sinuosity is widely used to identify areas based on tectonic activity. SMF index reflects a balance between the tendency of streams and slope processes to produce an irregular (sinuous) mountain front and vertical active tectonics that tends to produce a prominent straight front (Bull & McFadden, 1977). The index was defined as:

$$SMF = L_{mf} / L_s \qquad \text{Eq. (1)}$$

where SMF is the mountain front sinuosity index, Lmf is the straight-line distance along a contour line (as measured along with the prominent break in slope along the foot of a mountain), and Ls is the true distance along the same contour line (Figure 2).

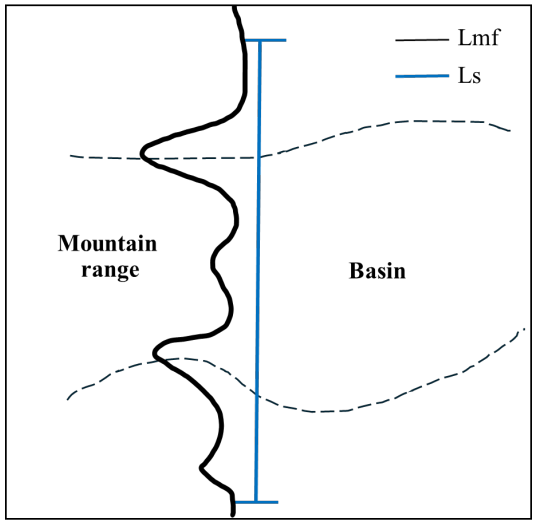

Figure 2. The method for calculation of SMF (Modified from Keller & Pinter, 2002).

2.2 Valley floor width-to-height ratio

The valley floor width to valley height ratio is an index based on tectonic activity. This index reflects the differences between the V-shaped valleys and U-shaped broad-floored valleys, which is a response to active uplift and indicates a relative of a base-level fall. The VF is defined as

$$VF = \frac{(2V_{fw} / L_s)}{[(E_{ld}-E_{sc})+(E_{rd}-E_{sc})]} \quad \text{Eq. (2)}$$

where VF is the valley floor width-to-height ratio index, V_{fw} is the width of the valley floor, E_{ld} and E_{rd} are the elevations of the left and right valley divides, respectively, and E_{sc} is the elevation of the valley floor (Figure 3).

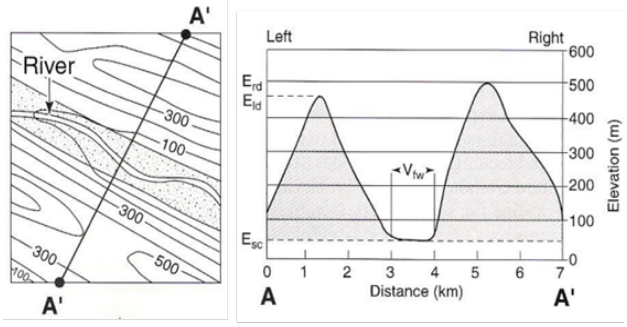

Figure 3. The method for calculation of VF ((Keller & Pinter, 2002) figure 4.15, p. 139).

2.3 Stream length gradient index

The Stream length gradient index is calculated along a river and used to evaluate the erosional resistance of the available rocks and the relative intensity of active tectonics. The SL index has a sensitivity to channel slope changes, which makes it a good evaluation tool for the relationship between potential tectonic activity, rock resistance, topography, and length of the stream. The index was defined as:

$$SL = (\Delta H / \Delta L) * L \quad \text{Eq. (3)}$$

where SL is the streaming length gradient, $\Delta H/\Delta L$ is the channel slope or gradient of a particular reach, ΔH is the change in elevation of the reach, ΔL is the length of the reach, and L is the total length from the midpoint of the reach of interest upstream to the highest point on the channel (Figure 4).

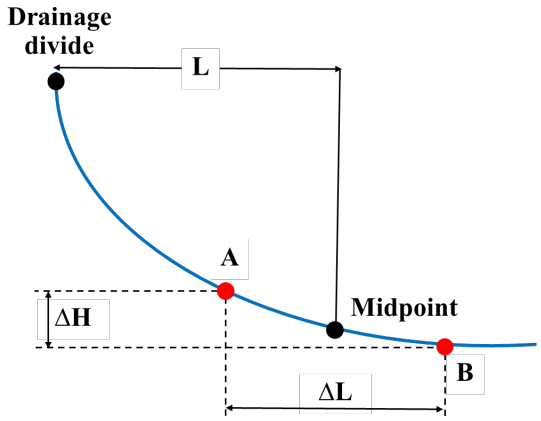

Figure 4. The method for calculation of SL along the stream (Modified from Hack, 1973).

2.4 Basin shape index

The basin shape index reflects that young drainage basins in active tectonic areas tend to be elongated in shape normal to the topographic slope of a mountain. In less active tectonic processes, the elongated shape tends to evolve to a more circular shape (Schumn, 1956). This index is defined as the ratio of the diameter of a circle in the same basin to the maximum basin length and is derived by the following formula:
Where BS is the basin shape index, B_l is the length of the basin measured from the headwaters point to the mouth, and B_w is the

width of the basin measured at the widest point (Figure 5).

2.5 Basin asymmetry index

The asymmetry factor was depicted in the flow of migrated rivers and the existence of tectonic tilting at the scale of a drainage basin. This method is mostly applied over a relatively large area (Hare and Gardner, 1985). and AF is defined by:

$$AF = 100^* (A_r / A_t) \qquad \text{Eq. (5)}$$

Where AF is the asymmetry factor, A_r is the area of the basin to the right, and A_t is the total area of the drainage basin. (Figure 6).

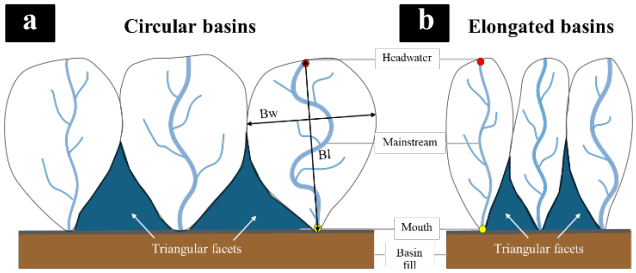

Figure 5. The method for calculation of BS and the drainage basin shape that is related to the active tectonic area: (a) circular basin response to less active tectonic, (b) elongated basin in active tectonic (Modified from Mahmood and Gloaguen, 2012).

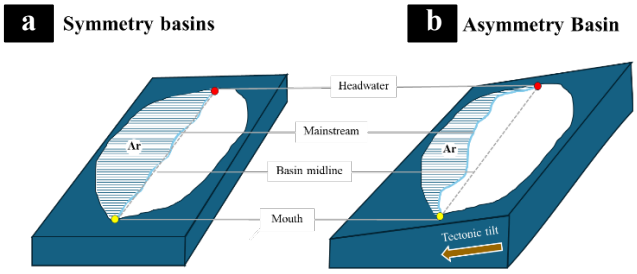

Figure 6. The method for calculation of AF, the drainage response to migrating and uplift along A fault: (a) symmetry basin response to less active tectonic, (b) asymmetry basin in active Tectonic (Modified from Mahmood and Gloaguen, 2012).

2.6 Basin hypsometric index

The hypsometry index is one of the most useful parameters that describe and analyze the distribution of elevations in an area (Pérez-Peña et al., 2009). The HI analysis has been used to differentiate between erosional landforms at different stages during their evolution (Strahler 1952; Schumm 1956). This index thus helps in explaining the erosion that had taken place in the watershed during the geological time scale due to hydrologic processes and land degradation factors (Bishop et al., 2003).

In addition, it is also an indication of the cycle of erosion, defined as the total time required for the reduction of a land topological unit to the base level, which is the lowest level. They are divided into three stages, i.e., the monadnock (old) stage, in which the watershed is fully stabilized and characterized by a landscape near base level with subdued relief. The equilibrium stage or mature stage is where many geographic processes operate in approximate equilibrium. In equilibrium or the early stage, the watershed is highly susceptible to erosion.

Strahler (1952) found that the characteristics of HI were inversely correlated with total relief, slope steepness, drainage density, and channel gradients. HI is expressed as a percentage and is an indicator of the remnant of the present volume as compared to the original volume of the basin (Ritter et al., 2007). This index is calculated by the following formula:

$$HI = \frac{E_{mean} - E_{min}}{E_{max} - E_{min}} \qquad \text{Eq. (6)}$$

Where E_{max} is the maximum elevation, E_{mean} is the mean elevation, and E_{min} is the minimum elevation of a drainage basin.

Moreover, the hypsometric curve is used together with HI by plotting to measure the distribution of the area concerning elevation in a basin. The curve is made from the proportion of basin area (a/A) and total basin elevation (h/H) where A is the total area, H is the highest elevation, a is the area of the basin at the height of h, and h is the height above outlet (Figure 7).

There are three types of the hypsometric curve, i.e., concave, convex, and S-shape (Strahler, 1952). The curve reflects the volume of rock mass in a basin and the amount of erosion that has taken place in a basin against the remaining mass (Farhan et al., 2016).

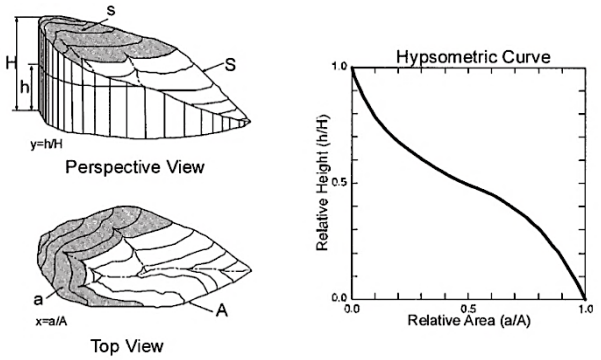

Figure 7. The diagram illustrates the hypsometric curve and the parameters involved. This curve essentially describes the distribution of area with elevation (Farhan et al., 2016).

3. Result

3.1. Mountain front sinuosity

The values of SMF were determined with 150 lineaments in different parts along the MCFZ and NMFZ. All the observed values ranged from 1.05 to 4.84. The mean value of the areas equals 1.81, and the minimum value is 1.05 (subbasin 32). In addition, the maximum value is 4.84 (subbasin 23).

The SMF values were recategorized for NMMC into five tectonic classes: class-1 (lesser active; SMF > 4.25), class-2 (active; 3.45 < SMF ≤ 4.25), class-3 (moderately active; 2.65 < SMF ≤ 3.45), class-4 (very active; 1.85 < SMF ≤ 2.65), and class-5 (highly active; < 1.85). Generally, Class 5 mostly occurred with structural zones in the northern and eastern areas of MCFZ and NMFZ (Table 1, Figure 8a).

3.2 Valley floor width-to-height ratio

In the present work, VF has been analyzed for various places along with the longitudinal profiles of all 76 valleys. The study found that the VF values ranging from 0.42 (subbasin 5) to 25.36 (subbasin 18). The VF has an average value of 5.03.

The VF values were recategorized for NMMC into five tectonic classes: class-1 (less active; VF ≥ 15.0), class-2 (weakly; 10.0 ≤ VF < 15.0), class-3 (moderately active; 5.0 ≤ VF < 10.0), class-4 (active; 2.0 ≤ VF < 5.0), and class-5 (highly active; ≤ 2.0). Most VF results are V-shaped valleys (class 5). and U-shaped valleys are in the southern part of the study area, which is Chiang Rai province (Table 1, Figure 8b).

3.3 Stream length gradient index

SL is calculated for all rivers in the basin to identify anomalous points that are reflected in the tectonic activity. The MCFZ and NMFZ can be divided into 12 stream orders, which contain a large number of the calculated SL points, around 88,500 points. All the observed average values range from 2,051 (subbasin 18) to 48,169 (subbasin 25). The SL has an average value of 13,228.

Consequently, the SL values were recategorized for NMMC into six tectonic classes: class-1 (lesser active; SL ≤ 9421), class-2 (active; 9421-17170), class-3 (moderately active; 17170-24920), class-4 (very active; 24920-32670), class-5 (extremely active; 32670–40419) and class-6 (exceptionally active; SL ≥ 40,419). Generally, the high additional values are represented as highly active caused by fault, lineament, and tectonic uplifting (Table 1, Figure 8c).

3.4 Basin shape index

The active basins crossing the faults will show an elongated basin, causing rapid uplifts with high values of BS. The study found that the BS values range from 1.01 (subbasin 28) to 3.33 (subbasin 4). The BS has an average value of 1.68.

Further, the computed BS values are divided into five active classes: class-1 (less active; BS < 1.53), class-2 (active; 1.53-2.05), class-3 (moderately active; 2.06–2.57), class-4 (very active; 2.58–3.09), and class-5 (highly active; BS > 3.09). Generally, the observed BS values in this study area are dominated by class 1 and class 2. It indicates these basins are circular.

However, only subbasin four was elongated in the basin by the reactivation of active faults between MCFZ and NMFZ (Table 1, Figure 8d).

3.5 Basin asymmetry index

Wide variations in AF values have been observed in the different parts of the basin. To determine tectonic tilt and avoid the possible intermingling of the outputs. The Results have a

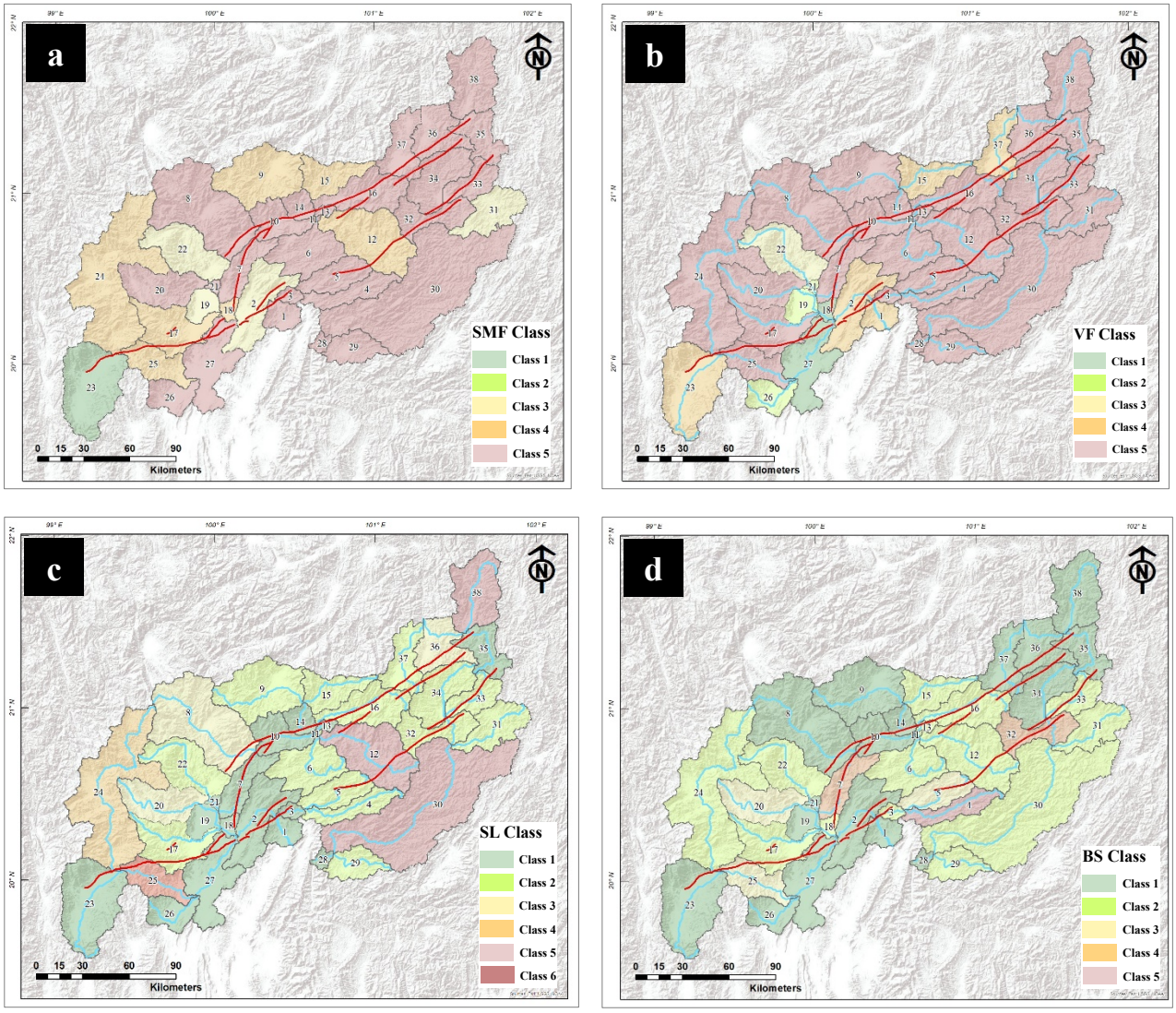

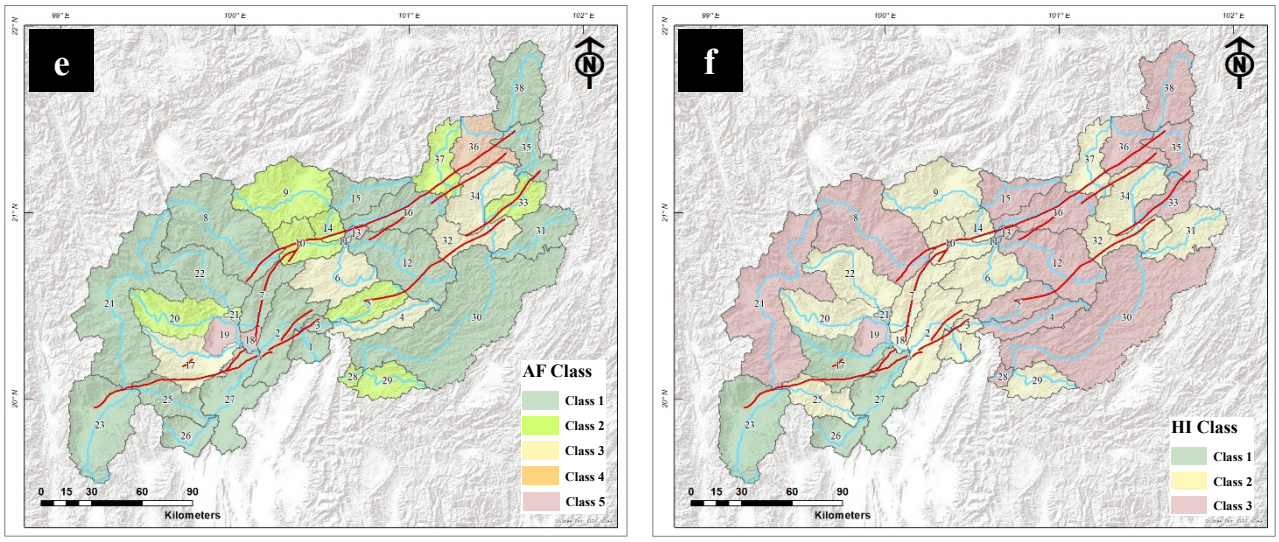

Figure 8. Map of MCFZ and NMFZ showing distribution result of the geomorphic index related to the tectonic activity. (a) SMF, (b) VF, (c) SL, (d) BS, (e) AF, and (f) HI index, respectively.

value range from 13.15 (subbasin 19) to 88.01 (subbasin 13). The mean value of AF for the NMMC equals 0.52.

Regarding ,Dubey et al. (2017) who proposed an analytical method based on the concept that if the area is tectonically stable, the AF values should equal 50. Therefore, the AF values obtained from this study will be subtracted from 50 before being compared and classified further. The degree of tectonic activity will depend on the AF values' deviation from 50, which were categorized into five tectonic classes: class-1 (less active; $-8.01 \leq AF \leq 8.01$), class-2 (active; ($8.01 < AF \leq 15.51$) and ($-15.1 \leq AF < -8.01$)), class-3 (moderately active; ($15.51 < AF \leq 23.01$) and ($-23.01 \leq AF < -15.51$)), class-4 (very active; ($23.01 < AF \leq 30.51$) and ($-30.51 \leq AF < -23.01$)), and class-5 (highly active; ($AF > 30.51$) and ($AF < -30.51$)) (Table 1, Figure 8e).

3.6 Basin hypsometric index

Based on Eq. (6), all types of profile curves have been observed as concave, convex, and convano-convex in the study area. The HI curves of the river in subbasins 3, 5, 6, 11, 12, 13, 15, 16, 20, 24, 28, 30, 31, 32, 33, 34, 35, 36, 37, and 38 show concaves in upper reaches and convex in lower reaches. Moreover, the rest are concave (Figure 9).

The computed value of HI in all 38 subbasins along the MCFZ and NMFZ ranges between 0.11 (subbasin 19) and 0.40 (subbasin 5 and 16). The mean value of HI equals 0.28. The HI values were recategorized for NMMC into three tectonic classes: class-1 (lesser active; $HI < 0.2$), class-2 (moderately active; HI 0.2-0.3), and class-3 (very active; $HI > 0.3$) (Table 1, Figure 8f).

In this study, the results of HI curves are consistent with HI values. All the HI values are below 0.5. It represents the mature to old-stage basins that have been more eroded and less impacted by active tectonics.

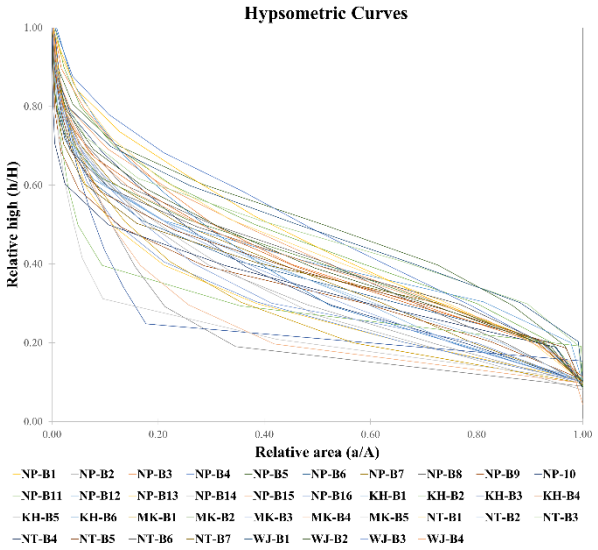

Figure 9. Hypsometric curves of the drainage basin in the MCFZ and NMFZ. Most graphs show concave.

4. Discussion

Spatial Variation of Relative Index of Active Tectonics (RIAT)

The RIAT was used to evaluate ongoing tectonic activity in a wider area by a combination of various geomorphic parameters. The averages of six measured parameters were used to assess the spatial variability in tectonic activity by computing the relative index of tectonic activity (RIAT).

The distribution map of the relative Index of active tectonic classes (RIAT) in MCFZ and NMFZ is shown in Figure 10, with color classification based: i) green indicates a very less active area, ii) pale green indicates a low active area, iii) yellow indicates an active area, iv) orange indicates a moderately active rea and v) red indicates a highly active area.

The values of the RIAT index are graded into three classes, as shown in Table 1, which shows the result of the classification for each subbasin to define the degree of active tectonics class-1: (inactive tectonic; RIAT < 2), class-2 (moderately active tectonic; $2 \leq$ RIAT < 3), and class 3 (very active tectonic ; $3 \leq$ RIAT < 4).

The area quantity can be sorted in descending order as follows: about 60.29% of

Table 1. Relative indices of active tectonic (RIAT) classes in MCFZ and NMFZ.

No.	Basin	Class of geomorphic indices						Sum	RIAT value	Class RIAT
		SMF	VF	SL	BS	AF	HI			
1	NP-B1	5	4	1	1	1	2	4	0.67	2
2	NP-B2	3	4	1	1	1	2	4	0.67	2
3	NP-B3	5	5	1	2	1	2	5	0.83	2
4	NP-B4	5	5	2	5	3	3	11	1.83	3
5	NP-B5	5	5	2	3	2	3	8	1.33	3
6	NP-B6	5	5	2	2	3	2	7	1.17	3
7	NP-B7	5	5	1	4	1	2	7	1.17	3
8	NP-B8	5	5	3	1	1	3	5	0.83	3
9	NP-B9	4	5	2	1	2	2	5	0.83	2
10	NP-B10	5	5	1	1	2	2	5	0.83	2
11	NP-B11	5	5	2	2	3	3	8	1.33	3
12	NP-B12	4	5	5	2	1	3	6	1.00	3
13	NP-B13	5	5	1	2	5	3	10	1.67	3
14	NP-B14	5	5	1	1	2	2	5	0.83	2
15	NP-B15	4	4	2	2	1	3	6	1.00	2
16	NP-B16	5	5	2	2	1	3	6	1.00	3

17	KH-B1	4	5	2	2	3	2	7	1.17	3
18	KH-B2	4	1	1	2	5	2	9	1.50	2
19	KH-B3	4	2	1	1	5	1	7	1.17	2
20	KH-B4	4	5	3	3	2	3	8	1.33	3
21	KH-B5	5	2	1	1	2	1	4	0.67	2
22	KH-B6	3	3	2	2	1	2	5	0.83	2
23	MK-B1	1	4	1	1	1	1	3	0.50	1
24	MK-B2	4	5	4	2	1	3	6	1.00	3
25	MK-B3	4	5	6	3	1	2	6	1.00	3
26	MK-B4	5	2	1	1	1	1	3	0.50	1
27	MK-B5	5	1	1	1	1	1	3	0.50	1
28	NT-B1	5	5	1	1	2	3	6	1.00	2
29	NT-B2	5	5	2	2	2	2	6	1.00	3
30	NT-B3	5	5	5	2	1	3	6	1.00	3
31	NT-B4	3	5	2	2	1	2	5	0.83	2
32	NT-B5	5	5	2	4	3	2	9	1.50	3
33	NT-B6	5	5	2	2	2	3	7	1.17	3
34	NT-B7	5	5	2	1	3	2	6	1.00	3
35	WJ-B1	5	5	1	1	1	3	5	0.83	2
36	WJ-B2	5	5	3	1	4	3	8	1.33	3
37	WJ-B3	5	4	2	1	2	2	5	0.83	2
38	WJ-B4	5	5	5	1	1	3	5	0.83	3

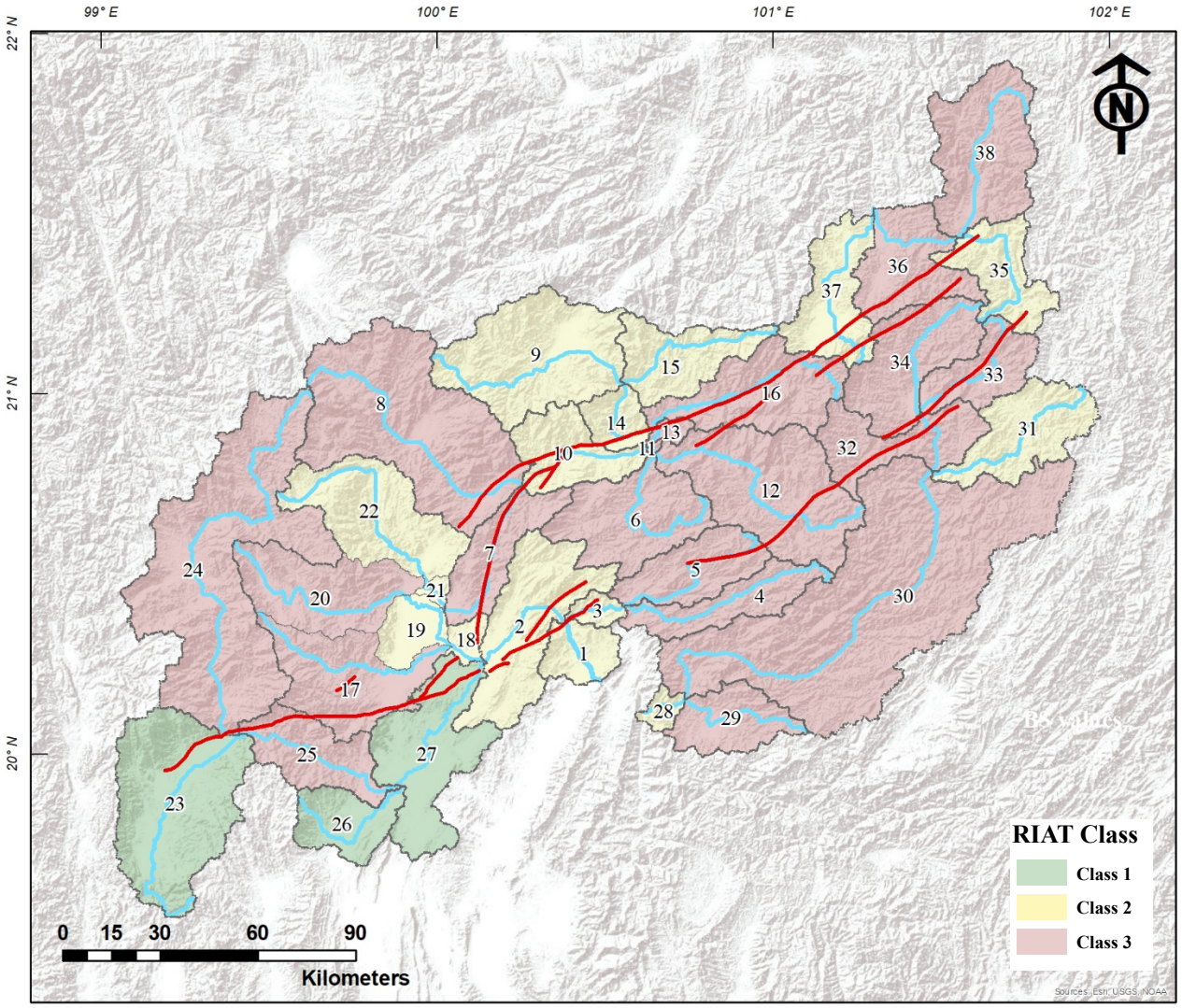

Figure 10. Distribution map of relative Index of active tectonic classes (RIAT) in MCFZ and NMFZ.

The basin covering ~22,827 km^2 is very active tectonic (class 3), about 34.92% of the basins covering 13.221 km^2 are very active tectonic (class 2), and about 4.79% of the basins covering 1,813 km^2 area is inactive tectonic.

5. Conclusion

The geomorphic indices are a useful tool for evaluating the effects of active tectonics in an area. These methods can be used as surveying instruments to detect the geomorphic anomalies related to tectonic activity. This is particularly valuable in the MCFZ and NMFZ, where very little work on the relation between neotectonics activity and geomorphology is available.

We used DEM 30 resolution with six geomorphic indices: mountain front sinuosity (SMF), valley floor width to height ratio (VF), stream length gradient index (SL), basin shape index (BS), basin asymmetry index (AF), and basin hypsometric index (HI). All the values of these indices were categorized into classes.

Furthermore, the results of geomorphic analysis, compared with the data of fault activity, show a good agreement. The response of rivers to individual fault structures is evident. According to the results, the values of SL percentage have been showing the anomalies point along the stream that were related to the influence of tectonic activity. Similar findings emerged from the calculation of SMF, which, according to the classification of Mulyasari and Brahmantyo (2017), is primarily of class 1 that mountain fronts are highly active. The calculated

values of the VF indicate that the majority of drainage basins have a V-shape. Moreover, AF shifted to the northwest of the drainage sub-watershed, whereas the Khong River has been displaced to the west, implying that the tectonic activity affects the evolution of this area. Although the hypsometric integral values of the basins in the study area vary between 0.11 and 0.40, indicate that the S-shaped curves indicate the basins are in a mature stage. The value of BS for the whole MCFZ and NMFZ indicates a circular basin shape that represents very little activity. Taking into account that the seismic record for the study area is low frequency, we can conclude finally that the combination of geomorphic and tectonic data provides a valuable tool for estimating the potential seismotectonic hazard in regions of low-rate active deformation.

Acknowledgments

We sincerely thank all staff at the Department of Geology, Faculty of Science, Chulalongkorn University, and the Department of Mineral Resource (DMR) for the great support, commendations, and suggestions to make this study successful.

References

Ahmad, S., Bhat, M. I., Madden, C., & Bali, B. S. (2014). Geomorphic analysis reveals active tectonic deformation on the eastern flank of the Pir Panjal Range, Kashmir Valley, India. *Arabian Journal of Geosciences*, *7*(6), Article 6.

Bishop, M. P., Shroder, J. F., & Colby, J. D. (2003). Remote sensing and geomorphometry for studying relief production in high mountains. *Geomorphology*, *55*(1–4), 345–361.

Bull, W. B. (2011). *Tectonically active landscapes*. John Wiley & Sons.

Bull, W. B., & McFadden, L. D. (1977). Tectonic Geomorphology North and South of the Garlock Fault, California. In *Geomorphology in Arid Regions*. Routledge.

Burbank, D. W., & Anderson, R. S. (2011). *Tectonic geomorphology*. John Wiley & Sons.

Clark, M. K., Schoenbohm, L. M., Royden, L. H., Whipple, K. X., Burchfiel, B. C., Zhang, X., Tang, W., Wang, E., & Chen, L. (2004). Surface uplift, tectonics, and erosion of eastern Tibet from large-scale drainage patterns. *Tectonics*, *23*(1).

Dubey, R. K., Dar, J. A., & Kothyari, G. C. (2017). Evaluation of relative tectonic perturbations of the Kashmir Basin, Northwest Himalaya, India: An integrated morphological approach. *Journal of Asian Earth Sciences*, *148*, 153–172.

El Hamdouni, R., Irigaray, C., Fernández, T., Chacón, J., & Keller, E. A. (2008). Assessment of relative active tectonics, southwest border of the Sierra Nevada (southern Spain). *Geomorphology*, *96*(1), 150–173.

Farhan, Y., Elgaziri, A., Elmaji, I., & Ali, I. (2016). Hypsometric Analysis of Wadi Mujib-Wala Watershed (Southern Jordan) Using Remote Sensing and GIS Techniques. *International Journal of Geosciences*, *07*(02), Article 02.

Hack, J. T. (1973). Stream-profile analysis and stream-gradient index. *Journal of Research of the U.S. Geological Survey*, *1*(4), 421–429.

Howard, A. D. (1967). Drainage analysis in geologic interpretation: A summation. *AAPG Bulletin*, *51*(11), 2246–2259.

Jackson, J., van Dissen, R., & Berryman, K. (1998). Tilting of active folds and faults in the Manawatu region, New Zealand: Evidence from surface drainage patterns.

New Zealand Journal of Geology and Geophysics, *41*(4), 377–385.

Keller, E. A., & Pinter, N. (1996). *Active tectonics* (Vol. 338). Prentice Hall Upper Saddle River, NJ.

Keller, E. A., & Pinter, N. (2002). *Active Tectonics: Earthquakes, Uplift, and Landscape*. Prentice Hall.

Morley, C. K. (2004). Nested strike-slip duplexes, and other evidence for Late Cretaceous–Palaeogene transpressional tectonics before and during India–Eurasia collision, in Thailand, Myanmar and Malaysia. *Journal of the Geological Society*, *161*(5), 799–812.

Morley, C. K. (2007). Variations in Late Cenozoic–Recent strike-slip and oblique-extensional geometries, within Indochina: The influence of pre-existing fabrics. *Journal of Structural Geology*, *29*(1), Article 1.

Mulyasari, R., & Brahmantyo, B. (2017). Morphometric analysis of relative tectonic activity in the Baturagung Mountain, Central Java, Indonesia. *IOP Conference Series: Earth and Environmental Science*, *71*(1), 012006.

Ornthammarath, T. (2012). A note on the strong ground motion recorded during the Mw 6.8 earthquake in Myanmar on 24 March 2011. *Bulletin of Earthquake Engineering*, *11*, 241–254.

Pérez-Peña, J., Azañón, J., Azor, A., Delgado, J., & Francisco, G. (2009). Spatial analysis of stream power using GIS: SLk anomaly maps. *Earth Surface Processes and Landforms*, *34*, 16–25.

Ritter, J. B., Rumschlag, J. H., & Zaleha, M. J. (2007). Evaluating Recent Stream Channel and Pattern Changes for Stream Resource Protection and Restoration: An Example from West-central Ohio. *Journal of Great Lakes Research*, *33*, 154–166.

Strahler, A. N. (1952). Hypsometric (area-altitude) analysis of erosional topography. *Geological Society of America Bulletin*, *63*(11), 1117–1142.